

## PATTERN FORMATION AND PERIODIC STRUCTURES IN SYSTEMS MODELED BY REACTION-DIFFUSION EQUATIONS

BY J. M. GREENBERG<sup>1</sup>, B. D. HASSARD AND S. P. HASTINGS<sup>1</sup>

**1. Introduction.** Excitable media are most often modeled by “reaction-diffusion” equations of the form

$$\partial \mathbf{u} / \partial t = \mathbf{F}(\mathbf{u}) + \Lambda \Delta \mathbf{u}. \quad (1.1)$$

$\mathbf{u}(\mathbf{x}, t)$  is an  $n$  vector which defines the state of the system at a given point  $\mathbf{x}$  at time  $t$ . The nonlinear function  $\mathbf{F}$  describes the “kinetics” of the medium while the diffusion effects enter via the term  $\Lambda \Delta \mathbf{u}$ .  $\Lambda$  is a diagonal matrix with nonnegative entries and  $\Delta$  is the Laplace operator in the appropriate number of space dimensions, in this paper one or two. In a spatially homogeneous configuration the state of the system evolves according to

$$d\mathbf{u} / dt = \mathbf{F}(\mathbf{u}). \quad (1.2)$$

The features which characterize “excitability” can be described in terms of this kinetic equation. They are (i) a globally stable equilibrium or rest state, (ii) an “excited” region of the state space which can be reached if a stimulus is applied to the system which exceeds some threshold level, and (iii) a refractory region of the state space in which the system will gradually return to rest, and will not respond to further stimulation unless sufficiently near the rest state. The behavior of a typical trajectory is summarized in Figure 1.1.

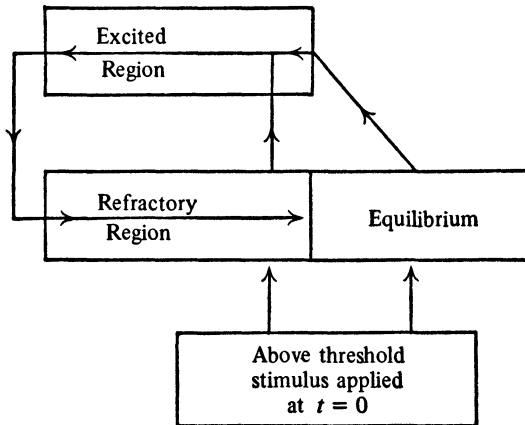


FIGURE 1.1

---

An invited address presented by Professor Greenberg at 81st Summer Meeting of the American Mathematical Society in Seattle, Washington on August 16, 1977; received by the editors October 19, 1977.

*AMS (MOS) subject classifications* (1970). Primary 34C25, 35B10, 35Q99, 92A15; Secondary 35C05, 34E99, 35A35, 39A10.

<sup>1</sup>The work of these authors was partially supported by the National Science Foundation.

© American Mathematical Society 1978

The striking feature of such media is that in a spatially inhomogeneous situation, where diffusion effects enter, they may settle into nonequilibrium modes which persist in time. In general these modes exhibit a high degree of spatial organization. This can be illustrated by considering two well known examples of “excitable” media, nerve tissue [4] and the Belousov-Zhabotinskiĭ reagent [8].

In the nerve axon, or “neural transmission line”, one observes that if a stimulus of sufficient intensity is applied to one end of the line, a pulse of electrical activity is generated which propagates along the line. Neither the shape nor the speed of propagation of this pulse seems to depend on the details of the end stimulus.

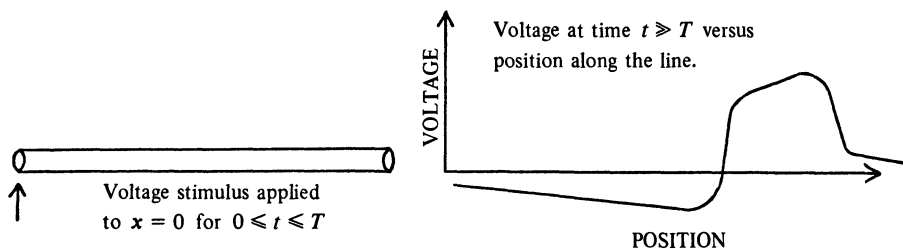


FIGURE 1.2

Similar phenomena are associated with the Belousov-Zhabotinskiĭ reaction. If a thin layer of the initially pink reagent is stimulated with a hot wire at a single point, a blue wave front is seen to spread outward from the point of stimulation. If the petri dish containing the reagent is then tilted, the wave is sheared and spiral wave fronts of blue appear. These spiral fronts rotate at a frequency which is a characteristic of the medium.

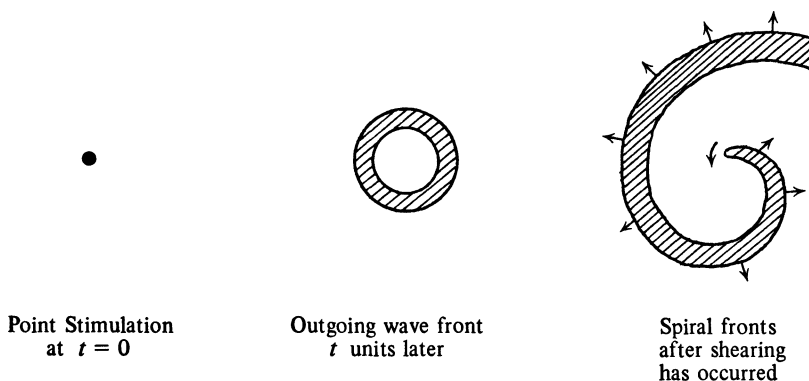


FIGURE 1.3

Our basic problem is to understand how the dynamical and diffusive terms interact to produce persistent, nonequilibrium solutions.

In §2 we shall consider a “discrete” model of an excitable system. Versions of this model have been considered by others (e.g. [6], [7]), usually in the context of cardiac irregularities. The “kinetics” of this model are based on the schematic of Figure 1.1 The underlying medium where the “reaction” takes

place is taken to be an array of square cells which interface with one another along horizontal or vertical boundaries. The model is mathematically tractable because of the simple mechanism which allows cells with a common boundary to communicate with one another. For this model a detailed analysis of the interaction of the kinetic and diffusive terms is possible. It is relatively easy to see how nonequilibrium solutions are established and maintain themselves. This model supports a wide variety of such solutions in both one and two space dimensions.

In §3 we turn to the original system (1) when the state space is  $R^2$ . In particular we consider

$$\varepsilon \partial u / \partial t = F(u, v) + \varepsilon^2 \Delta u \quad \text{and} \quad \partial v / \partial t = G(u, v) + \varepsilon^2 \lambda \Delta v \quad (1.3)$$

where  $0 < \varepsilon \ll 1$  and  $\lambda$ ,  $F$ , and  $G$  are independent of the small parameter  $\varepsilon$ . The equations describing nerve axon and the Belousov-Zhabotinskiï reagent are of the form (1.3). We first give a brief analysis of the spatially homogeneous version of these equations:

$$\varepsilon du/dt = F(u, v) \quad \text{and} \quad dv/dt = G(u, v). \quad (1.4)$$

We restrict our attention to smooth functions  $F$  and  $G$  satisfying hypotheses consistent with (i)–(iii). Then, we turn to the full system (1.3). An integration scheme for these equations which exploits the hypothesis  $0 < \varepsilon \ll 1$  is presented. We are able to show that these approximating equations support persistent nonequilibrium solutions of the desired type.

Strictly speaking, the approximating equations are just a more refined discrete model of an excitable medium. The reason for this is we do not have error estimates linking solutions of these equations to solutions of (1.3). Nevertheless, we feel that the scalings employed to derive these approximations are physically reasonable. These approximating equations are similar in structure to the discrete model considered in §2.

## 2. Discrete models.

2.1 *Spatially homogeneous processes.* We begin with the spatially homogeneous case. The state of the system at time  $t$  will be described by a scalar or phase  $u = u^t$ . Both  $t$  and  $u$  are discrete.  $u$  takes values from a fixed set

$$\mathfrak{S} = \{0, 1, 2, \dots, e, e + 1, e + 2, \dots, e + r\}$$

of nonnegative integers and  $t = 0, 1, 2, \dots$ . Elements of the subset  $\{1, 2, \dots, e\}$  will be identified as the “excited” states, elements of the subset  $\{e + 1, e + 2, \dots, e + r\}$  as the “refractory” states, and the singleton  $\{0\}$  as the “rest” or “equilibrium” state. We shall assume throughout that  $r > e$ . This property models the observation that the refractory phase is of longer duration than the excited phase for real excitable media. The dynamics of the model are specified by the rule

$$u^{t+1} = \mathfrak{E}(u^t), \quad (2.1)$$

where

$$\mathfrak{E}(k) = k + 1, \quad 1 < k < e + r - 1 \quad \text{and} \quad \mathfrak{E}(e + r) = \mathfrak{E}(0) = 0. \quad (2.2)$$

For any initial condition, after at most  $e + r$  time steps,  $u$  will arrive and

subsequently remain at zero. The state of rest is a globally stable equilibrium point for this model.

2.2 *Spatially inhomogeneous process.* We now augment this model to account for the presence of spatial inhomogeneities. We consider a two dimensional setting and partition the plane into square cells. The  $(i, j)$ th cell,  $C_{i,j}$ , is that unit square whose lower left-hand corner has the integer coordinates  $(i, j)$ .

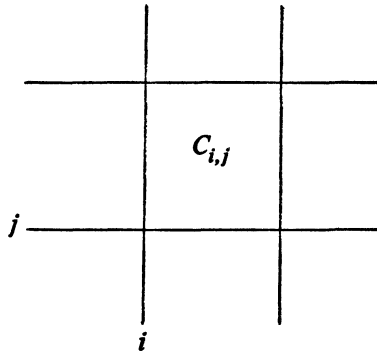


FIGURE 2.1

Let  $u'_{i,j} \in \mathcal{S}$  denote the state of the cell  $C_{i,j}$  at time  $t$ . Then, the state of  $C_{i,j}$  at time  $t + 1$ ,  $u'^{t+1}_{i,j}$ , is given by

$$u'^{t+1}_{i,j} = \mathcal{G}(u'_t) + \mathcal{D}(u'_t; u'_{i-1,j}, u'_{i,j-1}, u'_{i+1,j}, u'_{i,j+1}). \tag{2.3}$$

$\mathcal{G}(\cdot)$  is the reaction term defined in (2.2) and  $\mathcal{D}(\cdot; \cdot, \cdot, \cdot, \cdot)$  the diffusion term which defines how the four adjacent cells  $C_{i',j'}$ ,  $|i - i'| + |j - j'| = 1$ , affect the cell  $C_{i,j}$  from one instant to the next. We take

$$\mathcal{D}(u; v_1, v_2, v_3, v_4) = \begin{cases} 1, & \text{if } u = 0 \text{ and } 1 < v_i \leq e \\ & \text{for some } i = 1, 2, 3, \text{ or } 4, \\ 0, & \text{otherwise.} \end{cases} \tag{2.4}$$

The diffusion mechanism together with the evolution equation implies that if  $C_{i,j}$  is not at rest, then it evolves according to its local dynamics, while if it is at rest, it becomes excited at the next instant if and only if at least one of the cells adjacent to it is excited.

This model, while very simple, exhibits a surprising variety of persistent nonequilibrium solutions. It is not new. Several authors did computer studies of its behavior in the context of studies of cardiac irregularities. In two preceding papers ([2] for  $e = r = 1$  and [3] for  $e + r \geq 3$ ) it has been analyzed reasonably thoroughly. Here we summarize the main results of this earlier work and give examples of some of the more interesting persistent nonequilibrium solutions.

2.3 *One dimensional solutions.* One dimensional solutions of (2.3) and (2.4) evolve according to the rule

$$u'_k{}^{t+1} = \mathcal{G}(u'_k) + \hat{D}(u'_k; u'_{k+1}, u'_{k-1}) \tag{2.5}$$

where

$$\hat{D}(u; v_1, v_2) = \begin{cases} 1, & \text{if } u = 0 \text{ and } 1 \leq v_i \leq e \\ & \text{for } i = 1 \text{ or } 2, \\ 0, & \text{otherwise.} \end{cases} \quad (2.6)$$

These equations are obtained from (2.3) and (2.4) by looking for solutions which are independent of the indices  $i$  or  $j$ .

The simplest initial-value problem is that generated by point-stimulation data. We seek a solution of (2.5) satisfying the initial-condition

$$u_k^0 = \begin{cases} 1, & k = 0, \\ 0, & \text{otherwise.} \end{cases}$$

The solution is given by

$$u_k^t = U(t + 1 - |k|) \quad t \geq 0, \quad (2.7)$$

where

$$U(j) = \begin{cases} j, & 0 \leq j \leq e + r, \\ 0, & \text{otherwise.} \end{cases} \quad (2.8)$$

The profile,  $U(\cdot)$ , is a “steady” solution of (2.5), that is, it satisfies

$$U(j) = \mathcal{E}(U(j - 1)) + \hat{D}(U(j - 1); U(j - 2), U(j)) \quad (2.5)_{st}$$

and also the start up condition

$$U(j) = 0 \text{ for } j \leq 0 \text{ and } U(1) = 1.$$

A graph of the solution for  $k \geq 0$  is shown in Figure 2.2.

This solution has the form of two outgoing waves, moving in opposite directions from the point of initial stimulation. Observe that for each  $k$ ,

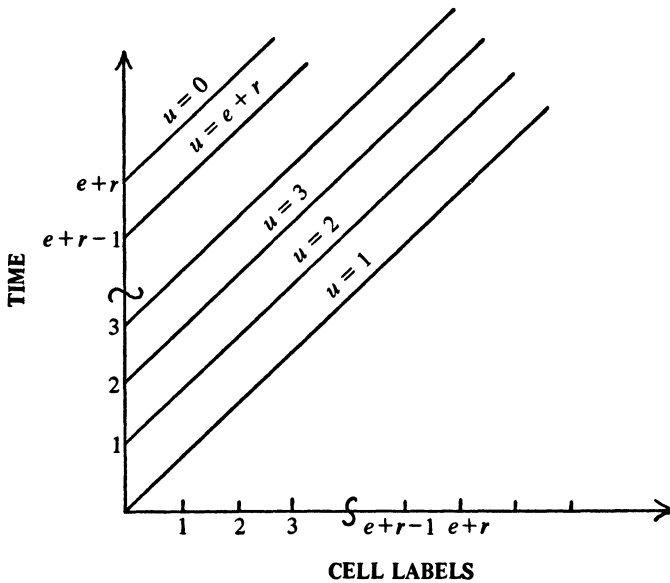


FIGURE 2.2

$\lim_{t \rightarrow \infty} u_k^t = 0$ , but this decay is not uniform in  $k$ .

On the other hand, some “nontrivial” initial data will decay uniformly. For example, choose an integer  $N > 0$  and let

$$u_k^0 = \begin{cases} |k| - N, & \text{if } N < |k| \leq N + e + r, \\ 0, & \text{otherwise.} \end{cases} \tag{2.9}$$

This generates two incoming waves, starting from  $k = \pm(N + 1)$ . When the waves “collide”, they are both destroyed, and  $u_k^t = 0$  for all  $k$  if  $t > N + e + r + 1$ .

In order to decide whether or not an initial pattern generates waves which die out uniformly, it is convenient to identify the state space  $\mathcal{S} = \{0, 1, \dots, e, e + 1, \dots, e + r\}$  with points on the unit circle in the complex plane, letting

$$\hat{\mathcal{S}} = \left\{ z = \exp\left(\frac{i2\pi k}{e + r + 1}\right), k = 0, 1, \dots, e + r \right\}. \tag{2.10}$$

Given points  $m$  and  $n$  in  $\mathcal{S}$ , we define the distance between  $m$  and  $n$ ,  $d(m, n)$ , by

$$d(m, n) = \min[|m - n|, e + r + 1 - |m - n|]. \tag{2.11}$$

It is easily checked that  $d(m, n)$  is also given by

$$d(m, n) = \frac{e + r + 1}{2\pi} \left[ \begin{array}{l} \text{length of the shortest arc on } |z| = 1 \\ \text{joining } \hat{m} = \exp\left(\frac{i2\pi m}{e + r + 1}\right) \text{ to } \hat{n} = \exp\left(\frac{i2\pi n}{e + r + 1}\right) \end{array} \right]. \tag{2.11}'$$

For convenience we assume that the initial data have finite support ( $u_k^0 = 0$  if  $|k|$  is sufficiently large) and satisfy the “continuity” condition

$$d(u_k^0, u_{k-1}^0) \leq e \text{ for all } k. \tag{2.12}$$

It is then not hard to show that for each  $t = 0, 1, 2, \dots$ , there is an  $M = M(t)$  such that  $u_k^t = 0$  if  $|k| \geq M$ , and also that  $d(u_k^t, u_{k-1}^t) \leq e$  for all  $t \geq 0$  and all  $k$ . We then define, for each  $t$ , a winding number  $W(u^t)$ , as the number of times the states  $\hat{u}_k^t = \exp(i2\pi u_k^t / (e + r + 1))$  wind around the circle  $|z| = 1$  as  $k$  goes from  $-M$  to  $M$ . An analytical formula for the winding number is given by

$$W(u^t) = \frac{1}{e + r + 1} \sum_{k=-M(t)}^{M(t)} \sigma(u_k^t, u_{k-1}^t) \tag{2.13}$$

where

$$\sigma(m, n) = \begin{cases} d(m, n), & \text{if the shortest arc joining } \hat{m} = \exp\left(\frac{i2\pi m}{e + r + 1}\right) \\ & \text{to } \hat{n} = \exp\left(\frac{i2\pi n}{e + r + 1}\right) \text{ is oriented counter-} \\ & \text{clockwise or if } \hat{m} \text{ and } \hat{n} \text{ are diametrically} \\ & \text{opposite each other,}^2 \\ -d(m, n), & \text{otherwise.} \end{cases} \tag{2.14}$$

<sup>2</sup>Note that  $e < r$  and (2.12) together prevent the diametrically opposite case from occurring in the flows  $u_k^t$  under consideration.

The basic result on decay or nondecay of solutions with finite support is then

**THEOREM 2.1.** *If the initial data  $u^0$  have finite support and satisfy the condition (2.12), then  $W(u^t) = W(u^0)$  for all  $t = 1, 2, 3, \dots$ . Furthermore,*

$$\lim_{t \rightarrow \infty} u_k^t = 0 \quad \text{for each } k,$$

and this decay is uniform in  $k$  only if  $W(u^0) = 0$ .

Solutions which do not decay even in the weak sense of this theorem are possible if the initial stimulus does not have finite support. There can be solutions such that  $\{t|u_k^t \neq 0\}$  is unbounded for each  $k$ . We call such solutions ‘‘persistent’’. Here we shall restrict our attention to spatially periodic initial data. It is then convenient to regard the evolution equations as holding on a circle

$$C_L = \{z = \exp(i2\pi k/L), k = 0, 1, 2, \dots, L - 1\}; \quad (2.15)$$

that is we take the neighbors of cell 0 to be cells 1 and  $L - 1$  and the neighbors of cell  $L - 1$  to be cells 0 and  $L - 2$ . Of course  $L > 0$  is the basic spatial period of the solution.

In this case the winding number should be defined slightly differently, by the relation

$$W_L(u^t) = \sum_{k=1}^L \sigma(u_k^t, u_{k-1}^t),$$

where we observe that  $u_L^t = u_0^t$  for all  $t$ . The result on persistence of solutions then takes the following form.

**THEOREM 2.2.** *Suppose that the initial data satisfy (2.12) and have period  $L$ . Then,  $W_L(u^t) = W_L(u^0)$  for all  $t \geq 0$ , and the solution is persistent if and only if  $W_L(u^0) \neq 0$ .*

The following examples illustrate the above theorem and point out that some sort of ‘‘continuity’’ hypothesis is needed.

The simplest nondecaying, spatially periodic solutions are traveling waves. These are obtained when  $L \geq e + r + 1$  and are given by

$$u_k^t = U_L(t \pm k - m) \quad (2.16)$$

where

$$U_L(j) = \begin{cases} j, & 0 \leq j \leq e + r, \\ 0, & e + r + 1 \leq j \leq L, \text{ and } U_L(j + L) = U_L(j). \end{cases} \quad (2.17)$$

For these solutions

$$W_L(u^t) \equiv 1 \quad \text{and} \quad d(u_k^t, u_{k-1}^t) \equiv 1 \leq e. \quad (2.18)$$

These traveling waves are time periodic with period  $\mathcal{T} = L$  and propagate with speed  $c = \pm 1$ .

The equations also support time periodic solutions when the spatial period satisfies  $L < e + r$ . These solutions all have common period  $\mathcal{T} = e + r + 1$

and average speed of propagation  $c_{Av} = \pm L/\mathcal{T}$ . The following data generate such a solution when  $L > r + 2$ :

$$u_k^0 = k, \quad 0 < k < L - 1. \tag{2.19}$$

For this solution

$$W_L(u^0) = 1 \tag{2.20}$$

and

$$\max_k d(u_k^0, u_{k-1}^0) = e + (r + 2 - L) \leq e. \tag{2.21}$$

The solution,  $u_k^t$ , corresponding to the data (2.19) has been dubbed a “caterpillar-wave” because the widths of the “excited” and “refractory” regions alternately expand and contract.

When  $(e + r + 1)/2 < L \leq r + 1$ , the data (2.19) generate a solution which decays to zero after  $e + r + 1$  units of time have elapsed. In this case the winding number is again unity but

$$\max_k d(u_k^0, u_{k-1}^0) = e + (r + 2 - L) \geq e + 1. \tag{2.22}$$

This example shows that a “continuity” hypothesis like (2.12) is required if solutions are to persist. On the other hand, when  $0 < L \leq e$ , the solution with the data (2.19) also decays. In this case the winding number is zero.

2.4 *Two dimensional patterns.* For the model (2.3) and (2.4) it is easy to simulate the experiment of applying a point stimulus to a petri dish filled with a thin layer of the Belousov-Zhabotinskii reagent. Simply start the center cell in the first excited state, 1, and all others at rest; that is consider the data

$$u_{i,j}^0 = \begin{cases} 1, & (i,j) = (0, 0), \\ 0, & \text{otherwise.} \end{cases} \tag{2.23}$$

This data produces an outgoing wave which travels at speed 1. The evolution of this wave is shown in Figure 2.3.

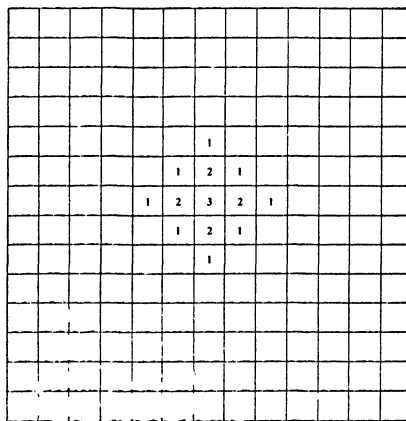


FIGURE 2.3

$t = 2$

All blank cells are in the state  $u = 0$ .



						1						
					1	·	1					
				1		·		1				
			1			$e+r-2$			1			
		1			$e+r-2$	$e+r-1$	$e+r-2$			1		
	1	·	·	$e+r-2$	$e+r-1$	$e+r$	$e+r-1$	$e+r-2$	·	·	1	
		1			$e+r-2$	$e+r-1$	$e+r-2$				1	
			1			$e+r-2$				1		
				1		·			1			
					1	·	1					
						1						

FIGURE 2.3.  $t = e + r - 1$ . All blank cells are in the state  $u = 0$ .

						1						
					1	·	1					
				1		·		1				
			1			$e+r-2$				1		
		1			$e+r-2$	$e+r-1$	$e+r-2$				1	
	1			$e+r-2$	$e+r-1$	$e+r$	$e+r-1$	$e+r-2$				1
1	·	·	$e+r-2$	$e+r-1$	$e+r$	0	$e+r$	$e+r-1$	$e+r-2$	·	·	1
	1			$e+r-2$	$e+r-1$	$e+r$	$e+r-1$	$e+r-2$				1
		1			$e+r-2$	$e+r-1$	$e+r-2$				1	
			1			$e+r-2$				1		
				1		·			1			
					1	·	1					
						1						

FIGURE 2.3.  $t = e + r$ . All blank cells are in the state  $u = 0$ .

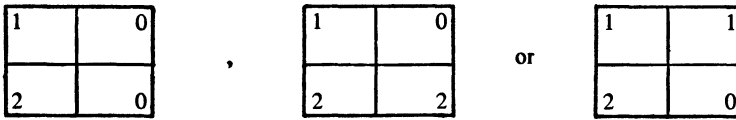
2.5 *Conditions for persistence of patterns.* The interesting new feature which appears in two dimensions is that some initial patterns,  $P^0$ , with only a finite number of nonzero cells generate solutions which do not decay.

We say that an initial pattern,  $P^0$ , generates a *persistent* solution if, for at least one pair  $(i, j)$ , the set

$$\mathfrak{T}_{i,j} \stackrel{\text{def}}{=} \{ t \geq 0 \mid u_{i,j}^t \neq 0 \} \tag{2.24}$$

is unbounded.<sup>3</sup> We shall give a condition which guarantees that a pattern generates such a solution. In addition, we shall give a necessary condition for persistence provided the initial pattern has only a finite number of nonzero cells.

The case where  $e = r = 1$  is quite simple. The result is that if the initial pattern contains one of the following three “cores” or “subpatterns”



or their mirror images or rotations, then the pattern will produce a persistent solution (for details see [2]).

Additional features appear when  $e + r \geq 3$ . We shall summarize the main results for this case. These are reported in detail in [3].

Our first result is

**THEOREM 2.3.** *If the initial pattern,  $P^0$ , contains only a finite number of nonzero cells and satisfies the condition<sup>4</sup>*

$$d(u_{i,j}^0, u_{i',j'}^0) < d_{\text{crit}} = \min\left(e + 1, \frac{e + r + 1}{4}\right) \tag{2.25}$$

for all adjacent cells  $C_{i,j}$  and  $C_{i',j'}$ , then the solution,  $u_{i,j}^t$ , of (2.3) and (2.4) dies out in any finite region in finite time; for any finite collection  $S$  of cells there is a time  $T(S)$  such that  $u_{i,j}^t = 0$  if  $C_{i,j} \in S$  and  $t \geq T(S)$ .

Theorem 2.3 gives the desired necessary condition for persistence, namely, that there be a “discontinuity” of sufficient strength in the initial pattern.

For a sufficient condition, we need the concept of a “cycle” of cells. Let  $m \geq 4$  be an integer. Then, a “cycle” is an ordered  $m$  tuple  $\mathcal{C} = (C^1, C^2, \dots, C^m)$  of distinct cells such that  $C^k$  is adjacent to  $C^{k+1}$  for  $1 \leq k \leq m - 1$  and  $C^m$  is adjacent to  $C^1$ .

Given any cycle  $\mathcal{C} = (C^1, C^2, \dots, C^m)$  and initial pattern  $P^0$  we let  $u_k^0$  be the state of cell  $C^k \in \mathcal{C}$  at  $t = 0$ . We define the winding number of the cycle  $\mathcal{C}$  relative to the pattern  $P^0$ ,  $W_{\mathcal{C}}(P^0)$ , as the number of times the states of the cycle wrap around the unit circle  $|z| = 1$  as the cycle is traversed. An analytical formula for  $W_{\mathcal{C}}(P^0)$  is given by

<sup>3</sup>This is equivalent to the condition that  $\mathfrak{T}_{i,j}$  is unbounded for all  $(i, j)$ .

<sup>4</sup>Again  $d(m, n) = \min[|m - n|, e + r + 1 - |m - n|]$  and cells  $C_{i,j}$  and  $C_{i',j'}$  are adjacent if and only if  $|i - i'| + |j - j'| = 1$ .

$$W_{\mathcal{C}}(P^0) = \frac{1}{e + r + 1} \sum_{k=1}^m \sigma(u_{k+1}^0, u_k^0) \tag{2.26}$$

where  $\sigma(\cdot, \cdot)$  is defined in (2.14) and  $u_{m+1}^0 = u_1^0$ .

The main result is

**THEOREM 2.4.** *If the initial pattern,  $P^0$ , contains a cycle  $\mathcal{C} = (C^1, C^2, \dots, C^m)$  satisfying*

$$d(u_{k+1}^0, u_k^0) \leq e, \quad k = 1, 2, \dots, m, \tag{2.27}$$

*then the resulting solution of (2.3) and (2.4) satisfies*

$$d(u_{k+1}^t, u_k^t) \leq e, \quad k = 1, 2, \dots, m, \tag{2.28}$$

and

$$W_{\mathcal{C}}(P^t) = W_{\mathcal{C}}(P^0), \quad t = 1, 2, \dots \tag{2.29}$$

*If moreover  $W_{\mathcal{C}}(P^0) \neq 0$ , then the solution is persistent.*

*Further, a solution  $P^t$ ,  $t > 0$ , with only a finite number of nonzero cells at  $t = 0$  is persistent if and only if there is a  $t_0 > 0$  and a cycle  $\mathcal{C}$  satisfying (2.28) at  $t = t_0$  and with  $W_{\mathcal{C}}(P^{t_0}) \neq 0$ .*

**2.6 Illustrative examples.** The first example shows how shearing a plane single pulse wave generates a rotating spiral wave. This illustrates Theorem 2.4. The second example, which illustrates Theorems 2.3 and 2.4, is motivated by the tilted petri disk experiment, the method used to generate rotating spirals in the Zhabotinskiĭ reagent. It shows how spirals can be generated by shearing an outgoing wave which is sufficiently well developed.

In the first example we take  $e = 2$  and  $r = 3$  and consider the initial pattern

$$u_{i,j}^0 = \begin{cases} -j + 1, & \text{if } -4 < j < 0 \text{ and } i \geq 0, \\ 0, & \text{otherwise.} \end{cases} \tag{2.30}$$

There are numerous cycles in this pattern. One is the cycle shown in Figure 2.4 at  $t = 0$ . This cycle satisfies the continuity condition (2.28) and has a winding number equal to unity. Thus, Theorem 2.4 guarantees that the pattern (2.30) generates a persistent solution. The evolution of this data is shown in Figure 2.4.

In the second example we again take  $e = 2$  and  $r = 3$ . Our data will be obtained from shearing the pattern shown in Figure 2.5. This particular pattern is the outgoing wave generated by the data

$$u_{i,j}^0 = \begin{cases} 1, & (i,j) = (0, 0), \\ 0, & \text{otherwise} \end{cases}$$

at  $t = 6$ . The sheared data is obtained from this pattern by shifting the rows  $j < -1$  to the right. Shifts of one or more units produce patterns with discontinuities satisfying  $d(u_{i,j}^0, u_{i',j'}^0) \geq d_{\text{crit}} = 2$  for some adjacent cells  $C_{i,j}$

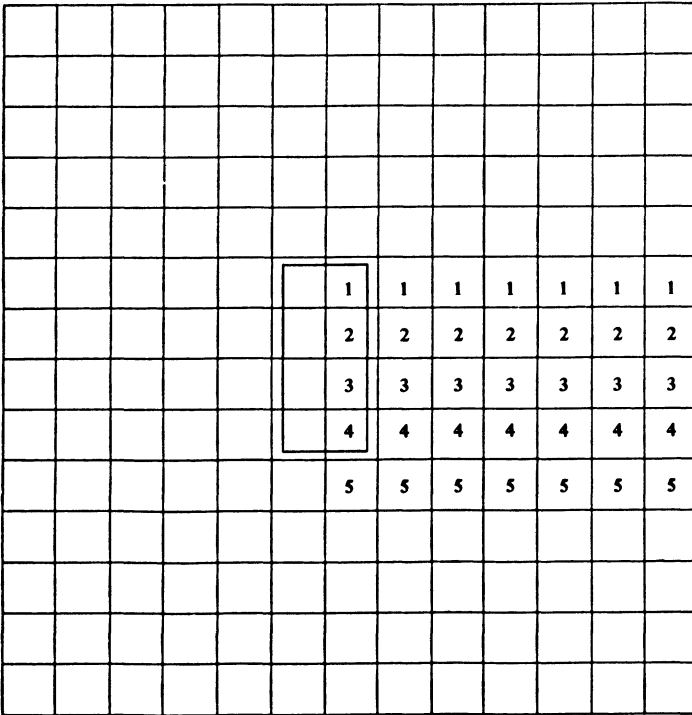


FIGURE 2.4.  $t = 0$ . All blank cells are in the state  $u = 0$ .

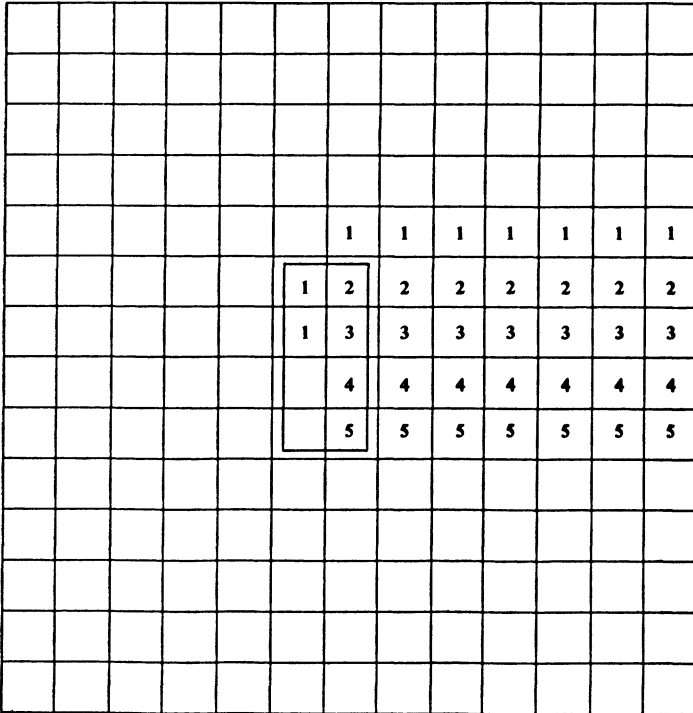


FIGURE 2.4.  $t = 1$  All blank cells are in the state  $u = 0$ .

						1	1	1	1	1	1	1
					1	2	2	2	2	2	2	2
				1	2	3	3	3	3	3	3	3
			1	2	3	4	4	4	4	4	4	4
			1	2	3	5	5	5	5	5	5	5
			1	2								
				1								

FIGURE 2.4.  $t = 3$ . All blank cells are in the state  $u = 0$ .

					1	2	2	2	2	2	2	2
				1	2	3	3	3	3	3	3	3
			1	2	3	4	4	4	4	4	4	4
		1	2	3	4	5	5	5	5	5	5	5
	1	2	3	4	5							
1	2	3	4	5		1						
1	2	3	4	5		2	1					
	1	2	3	4	5	3	2	1				
		1	2	3	4	3	2	1				
			1	2	3	2	1					
				1	2	1						
					1							

FIGURE 2.4.  $t = 6$ . All blank cells are in the state  $u = 0$ .

		1	2	3	4	5	5	5	5	5	5	5
	1	2	3	4	5							
1	2	3	4	5		1						
2	3	4	5		1	2	1					
3	4	5		1	2	3	2	1				
4	5		1	2	3	4	3	2	1			
4	5		1	2	3	5	4	3	2	1		
3	4	5		1	2		5	4	3	2	1	
2	3	4	5		1		5	4	3	2	1	
1	2	3	4	5		5	4	3	2	1		
	1	2	3	4	5	4	3	2	1			
		1	2	3	4	3	2	1				
			1	2	3	2	1					
				1	2	1						

FIGURE 2.4.  $\tau = 9$ . All blank cells are in the state  $u = 0$ .

2	3	4	5		1	2	1						
3	4	5		1	2	3	2	1					
4	5		1	2	3	4	3	2	1				
5		1	2	3	4	5	4	3	2	1			
	1	2	3	4	5		5	4	3	2	1		
1	2	3	4	5		1		5	4	3	2	1	
1	2	3	4	5		2	1		5	4	3	2	
	1	2	3	4		5	3	2	1		5	4	3
5		1	2	3		4	3	2	1		5	4	3
4	5		1	2		3	2	1		5	4	3	2
3	4	5		1		2	1		5	4	3	2	1
2	3	4	5			1		5	4	3	2	1	
1	2	3	4	5			5	4	3	2	1		
	1	2	3	4		5	4	3	2	1			

FIGURE 2.4.  $\tau = 12$ . All blank cells are in the state  $u = 0$ .

						1						
					1	2	1					
				1	2	3	2	1				
			1	2	3	4	3	2	1			
		1	2	3	4	5	4	3	2	1		
	1	2	3	4	5	0	5	4	3	2	1	
1	2	3	4	5	0	0	0	5	4	3	2	1
	1	2	3	4	5	0	5	4	3	2	1	
		1	2	3	4	5	4	3	2	1		
			1	2	3	4	3	2	1			
				1	2	3	2	1				
					1	2	1					
						1						

FIGURE 2.5. All blank cells are in the state  $u = 0$ .

						1						
						1	2	1				
					1	2	3	2	1			
				1	2	3	4	3	2	1		
		1	2	3	4	5	4	3	2	1		
	1	2	3	4	5	0	5	4	3	2	1	
1	2	3	4	5	0	0	0	5	4	3	2	1
				1	2	3	4	5	0	5	4	3
					1	2	3	4	5	4	3	2
						1	2	3	4	3	2	1
							1	2	3	2	1	
								1	2	1		
									1			

FIGURE 2.6. All blank cells are in the state  $u = 0$ .

and  $C_{i,j}$ , and thus such data has a chance of producing persistent solutions. Shifts of less than three units yield no continuous cycles with nonzero winding numbers. A shift of three units yields a pattern with two nonoverlapping cycles, each with nonzero winding number and each satisfying (2.27) (see Figure 2.6). Each of these cycles forms the core of a spiral.

We conclude that the initial outgoing wave shows a kind of stability in that a small distortion will not produce a large enough discontinuity to allow for persistence. On the other hand, once a persisting pattern is created, it is stable as well, since a random change in the pattern at any  $t$  is unlikely to destroy all continuous cycles or change their winding numbers to 0.

**3. Two-dimensional reaction-diffusion equations.** In this section we examine the behavior of the system

$$\begin{cases} \epsilon \frac{\partial u}{\partial t} = F(u, v) + \epsilon^2 \Delta u, & \text{and} \\ \frac{\partial v}{\partial t} = G(u, v) + \epsilon^2 \lambda \Delta v. \end{cases} \tag{3.1}$$

**3.1 Spatially homogeneous equations.** Our first task is to analyze briefly the spatially homogeneous version of (3.1), i.e.

$$\begin{cases} \epsilon \frac{du}{dt} = F(u, v), & \text{and} \\ \frac{dv}{dt} = G(u, v). \end{cases} \tag{3.2}$$

Our interest is in the case where  $0 < \epsilon \ll 1$ . The functions  $F$  and  $G$  are smooth and satisfy

- (A-1) the point  $(u, v) = (0, 0)$  is the unique solution of  $(F, G) = (0, 0)$ ,
- (A-2)  $F_v < 0$ ,  $G_u > 0$ , and  $G_v \leq 0$  for all  $u$  and  $v$ , and
- (A-3)  $F(\cdot, 0)$  has exactly three zeros, namely  $u = 0$ ,  $u = a \in (0, 1)$ , and  $u = 1$ , and  $F_u(0, 0) < 0$ ,  $F_u(a, 0) > 0$ , and  $F_u(1, 0) < 0$ .

One such pair  $(F, G)$  is given by

$$F = u(u - a)(1 - u) - v \quad \text{and} \quad G = u - Kv \tag{3.3}$$

where

$$0 < K < 4/(1 - a)^2 \quad \text{and} \quad 0 < a < 1/2. \tag{3.4}$$

The system (3.1) with  $F$  and  $G$  given by (3.3) was used by FitzHugh [1] and Nagumo, Arimoto, and Yoshizawa [5] to model voltage transmission along a nerve axon.

There are a number of implications of the hypotheses (A-1)–(A-3). We summarize them below:

There is a smooth, nondecreasing function  $g(\cdot)$  satisfying  $G(g(v), v) = 0$ ,  $-\infty < v < \infty$ , and a smooth function  $f(\cdot)$  satisfying  $F(u, f(u)) = 0$ .  $f$  has exactly the same zeros as  $F(\cdot, 0)$  and  $f'(0) < 0$ ,  $f'(a) > 0$ , and  $f'(1) < 0$ .

In what follows we shall let  $v_{\min}$  and  $v_{\max}$  denote the minimum and



maximum values of  $f(\cdot)$  on  $(0, 1)$ . We shall assume

(A-4) There are unique points  $u_{\min}$  and  $u_{\max}$  such that  $f(u_{\min}) = v_{\min}$  and  $f(u_{\max}) = v_{\max}$ .

These points satisfy  $0 < u_{\min} < a < u_{\max} < 1$ . We shall also assume

(A-5)  $f'' \leq 0$  on  $u < u_{\min}$  and  $f'' \geq 0$  on  $u > u_{\max}$ .

The relevant information about the curves  $u = g(v)$  and  $v = f(u)$  is summarized in Figure 3.1.

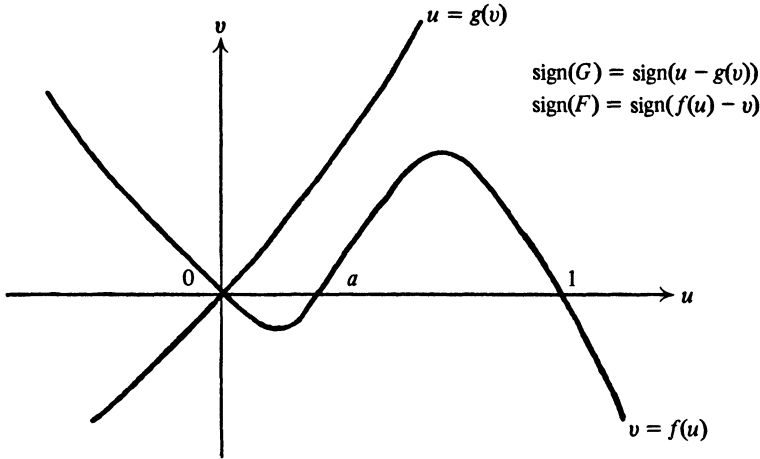


FIGURE 3.1

We are now in a position to describe the phase plane associated with (3.2). We discuss the singular case when  $\varepsilon = 0^+$  first. We introduce the “switch” curve

$$v = S(u) \stackrel{\text{def}}{=} \begin{cases} v_{\min}, & u \leq u_{\min}, \\ f(u), & u_{\min} < u < u_{\max}, \\ v_{\max}, & u_{\max} < u. \end{cases} \quad (3.5)$$

For initial points  $(u_0, v_0)$  where  $v_0 \geq S(u_0)$ , the singular flow jumps instantaneously to the point  $(u_1, v_0)$  where  $v_0 = f(u_1)$ ,  $u_1 \leq u_{\min}$  and then proceeds monotonically along the curve  $v = f(u)$ ,  $u \leq u_{\min}$  into the origin as  $t \rightarrow \infty$ . For initial points  $(u_0, v_0)$  where  $v_0 < S(u_0)$ , the singular flow jumps instantaneously to the point  $(u_1, v_0)$  where  $v_0 = f(u_1)$ ,  $u_1 > u_{\max}$ , and then proceeds along the curve  $v = f(u)$ ,  $u \geq u_{\max}$  to the point  $(u_{\max}, v_{\max})$ . From  $(u_{\max}, v_{\max})$  the flow jumps instantaneously to the point  $(u_2, v_{\max})$  where  $v_{\max} = f(u_2)$ ,  $u_2 < 0$  and then proceeds to the origin along the curve  $v = f(u)$ ,  $u < 0$ , as  $t \rightarrow \infty$ . The switch curve defines the threshold for the singular system. The excited states,  $E$ , are given by

$$E = \{(u, f(u)) | u_{\max} < u\} \quad (3.6)$$

and the refractory states,  $R$ , by

$$R = \{(u, f(u)) | u < u_{\min}\}. \quad (3.7)$$

The trajectories associated with (3.2) when  $0 < \varepsilon \ll 1$  differ little from those of the singular case, shown in Figure 3.2.

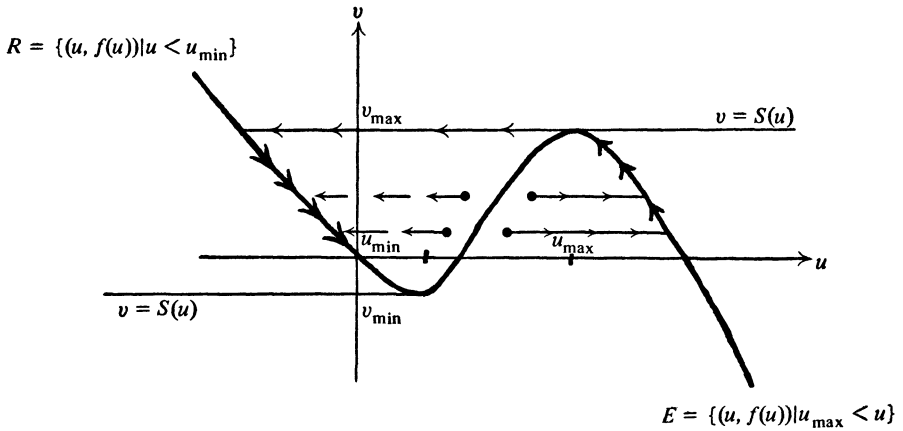


FIGURE 3.2

3.2 *The integration scheme.* We now turn to the full system (3.1). We shall develop and analyze an integration scheme for this system. The scheme will be derived in the two-dimensional case, the one-dimensional scheme arising when the data is independent of one of the space variables.

We replace the continuous space variable  $(x, y)$  by  $(x_i, y_j) = (ih, jh)$  and the Laplace operator  $\Delta u(x, y)$  by  $h^{-2}Du_{i,j}$  where

$$Du_{i,j} = (u_{i-1,j} + u_{i,j-1} + u_{i+1,j} + u_{i,j+1} - 4u_{i,j}). \tag{3.8}$$

Here, we have replaced  $u(ih, jh)$  by  $u_{i,j}$ . Under these substitutions (3.1) goes into

$$\begin{cases} \epsilon \frac{du_{i,j}}{dt} = F(u_{i,j}, v_{i,j}) + \left(\frac{\epsilon}{h}\right)^2 Du_{i,j}, & \text{and} \\ \frac{dv_{i,j}}{dt} = G(u_{i,j}, v_{i,j}) + \lambda \left(\frac{\epsilon}{h}\right)^2 Dv_{i,j}. \end{cases} \tag{(3.1)_{i,j}}$$

We now introduce a “local” integration scheme to advance the solution from time  $t_n \stackrel{\text{def}}{=} n\delta$  to  $t_{n+1} \stackrel{\text{def}}{=} (n+1)\delta$ . A “fractional-step” method will be used. In computing the intermediate step,  $(U_{i,j}^{n+1}, V_{i,j}^{n+1})$ , at  $t_{n+1}$  we allow the “fast” variable  $u$  to diffuse and the “slow” variable  $v$  to both react and diffuse. The result of this computation is

$$U_{i,j}^{n+1} = \mu(u_{i-1,j}^n + u_{i,j-1}^n + u_{i+1,j}^n + u_{i,j+1}^n) + (1 - 4\mu)u_{i,j}^n, \tag{3.9}$$

and

$$\begin{aligned} V_{i,j}^{n+1} &= \Lambda(v_{i-1,j}^n + v_{i,j-1}^n + v_{i+1,j}^n + v_{i,j+1}^n) \\ &\quad + (1 - 4\Lambda)v_{i,j}^n + \delta G(u_{i,j}^n, v_{i,j}^n), \end{aligned} \tag{3.10}$$

where

$$\mu = \epsilon\delta/h^2 \text{ and } \Lambda = \mu\lambda\epsilon = \lambda\epsilon^2\delta/h^2. \tag{3.11}$$

These formulas are obtained by applying a first order Euler scheme to the initial-value problem (3.12) and (3.13):

$$\begin{cases} \epsilon \frac{dU_{ij}}{dt} = \left(\frac{\epsilon}{h}\right)^2 DU_{ij}, & \text{and} \\ \frac{dV_{ij}}{dt} = \lambda \left(\frac{\epsilon}{h}\right)^2 DV_{ij} + G(U_{ij}, V_{ij}) \end{cases} \quad (3.12)$$

$$(U_{ij}, V_{ij})(t_n) = (u_{ij}^n, v_{ij}^n) \quad (3.13)$$

and setting

$$(U_{ij}^{n+1}, V_{ij}^{n+1}) \stackrel{\text{def}}{=} (U_{ij}, V_{ij})(t_{n+1}). \quad (3.14)$$

To complete the advancement of the approximate solution to  $t_{n+1}$  we must still solve

$$\frac{du}{ds} = F(u, V_{ij}^{n+1}), \quad (3.15)$$

and

$$u(0) = U_{ij}^{n+1}. \quad (3.16)$$

At time  $t_{n+1}$ , the approximate solution  $(u_{ij}^{n+1}, v_{ij}^{n+1})$ , would then be given by

$$(u_{ij}^{n+1}, v_{ij}^{n+1}) = (u(\delta/\epsilon, U_{ij}^{n+1}, V_{ij}^{n+1}), V_{ij}^{n+1}). \quad (3.17)$$

For  $0 < \epsilon \ll 1$ , the problem (3.15) and (3.16) must be solved over large time intervals  $0 \leq s \leq \delta/\epsilon$  and to do this accurately at each mesh point would be impractical. Instead we exploit the smallness of  $\epsilon$ , that is the largeness of  $\delta/\epsilon$ , and replace  $u(\delta/\epsilon, U_{ij}^{n+1}, V_{ij}^{n+1})$  by  $\lim_{s \rightarrow \infty} u(s, U_{ij}^{n+1}, V_{ij}^{n+1})$ . The result of this replacement is

$$u_{ij}^{n+1} = \begin{cases} U_E(v_{ij}^{n+1}), & v_{ij}^{n+1} < S(U_{ij}^{n+1}), \\ U_R(v_{ij}^{n+1}), & v_{ij}^{n+1} \geq S(U_{ij}^{n+1}). \end{cases} \quad (3.18)$$

For  $v < v_{\max}$ ,  $U_E(v)$  is the largest solution of  $f(u) = v$ , while for  $v > v_{\min}$ ,  $U_R(v)$  is the smallest solution of  $f(u) = v$ . For  $v \in (v_{\min}, v_{\max})$ , the equation has an intermediate solution,  $U_I(v)$ . These roots satisfy

$$\begin{cases} U_R(v) < U_I(v) < U_E(v), \\ \frac{dU_E}{dv} < 0, \quad \frac{dU_R}{dv} < 0, \quad \text{and} \quad \frac{dU_I}{dv} > 0. \end{cases} \quad (3.19)$$

A summary of the integration scheme in one and two dimensions is given below:

$$\begin{cases} U_i^{n+1} = \mu(u_{i-1}^n + u_{i+1}^n) + (1 - 2\mu)u_i^n, \\ v_i^{n+1} = \Lambda(v_{i-1}^n + v_{i+1}^n) + (1 - 2\Lambda)v_i^n + \delta G(u_i^n, v_i^n), \quad \text{and} \\ u_i^{n+1} = \begin{cases} U_E(v_i^{n+1}), & v_i^{n+1} < S(U_i^{n+1}), \\ U_R(v_i^{n+1}), & v_i^{n+1} \geq S(U_i^{n+1}), \end{cases} \end{cases} \quad (3.20)$$

and

$$\left\{ \begin{aligned} U_{ij}^{n+1} &= \mu(u_{i-1j}^n + u_{ij-1}^n + u_{i+1j}^n + u_{ij+1}^n) + (1 - 4\mu)u_{ij}^n, \\ v_{ij}^{n+1} &= \Lambda(v_{i-1j}^n + v_{ij-1}^n + v_{i+1j}^n + v_{ij+1}^n) \\ &\quad + (1 - 4\Lambda)v_{ij}^n + \delta G(u_{ij}^n, v_{ij}^n), \text{ and} \\ u_{ij}^{n+1} &= \begin{cases} U_E(v_{ij}^{n+1}), & v_{ij}^{n+1} < S(U_{ij}^{n+1}), \\ U_R(v_{ij}^{n+1}), & v_{ij}^{n+1} > S(U_{ij}^{n+1}). \end{cases} \end{aligned} \right. \tag{3.21}$$

The parameters  $\mu, \delta, \epsilon,$  and  $\Lambda$  may be regarded as independent, and the ratio  $\delta/\epsilon$  should be large. The mesh spacing  $h$  and diffusion constant  $\lambda$  may be computed from these parameters by (3.11).

Throughout the remainder of this paper we shall restrict our attention to the case where

$$F = f_a(u) - v \quad \text{and} \quad G = u - Kv \tag{3.22}$$

where  $f_a(\cdot)$  is one of the two functions:

$$f_a(u) = u(u - a)(1 - u) \quad \text{or} \\ f_a(u) = \begin{cases} -au, & u < u_{\min} = a(1 - a)/(2 - a), \\ (1 - a)(1 - u), & u > u_{\max} = (1 + a^2)/(1 + a), \\ a(1 - a)(u - a), & u_{\min} < u < u_{\max}. \end{cases} \tag{3.23}$$

We assume that  $0 < a < 1/2$  and that  $0 < K$  is small enough so that the equations  $0 = u - Kv$  and  $0 = f_a(u) - v$  have  $(u, v) = (0, 0)$  as their only solution. For the cubic this is achieved by taking  $K < 4/(1 - a)^2$  while for the piecewise linear function it is achieved by taking  $K < 1/a(1 - a)$ . It should be noted that the piecewise linear function is modeled on the cubic. That is, both have the same derivatives at their common zeros.

Our results apply to more general functions  $F$  and  $G$  satisfying (A-1)–(A-5). Our reason for restricting ourselves to these cases is that it is easier to state parameter constraints.

**3.3 One dimensional problems.** In this subsection we shall deal exclusively with the one dimensional system

$$\left\{ \begin{aligned} U_i^{n+1} &= \mu(u_{i-1}^n + u_{i+1}^n) + (1 - 2\mu)u_i^n, \\ v_i^{n+1} &= \Lambda(v_{i-1}^n + v_{i+1}^n) + (1 - 2\Lambda)v_i^n + \delta G(u_i^n, v_i^n), \text{ and} \\ u_i^{n+1} &= \begin{cases} U_E(v_i^{n+1}), & v_i^{n+1} < S(U_i^{n+1}), \\ U_R(v_i^{n+1}), & v_i^{n+1} > S(U_i^{n+1}) \end{cases} \end{aligned} \right. \tag{3.20}$$

where  $F$  and  $G$  are given by (3.22).

Some tuning of the parameters  $\mu, \Lambda$  and  $\delta$  is necessary. We insist that

$$0 < \delta < a/(1 + Ka). \tag{3.24}$$

Then, we can be assured that  $(u, v) = (0, 0)$  is the only constant solution of the “homogeneous” system

$$\begin{aligned}
 v^{n+1} &= v^n + \delta G(u^n, v^n) \quad \text{and} \\
 u^{n+1} &= \begin{cases} U_E(v^{n+1}), & v^{n+1} < S(u^n), \\ U_R(v^{n+1}), & v^{n+1} \geq S(u^n), \end{cases} \tag{3.25}
 \end{aligned}$$

and that this point is “globally-asymptotically” stable. Later, we shall require additional constraints on  $\delta$ .

We shall assume throughout the remainder of this section that  $\mu \leq \frac{1}{2}$  and  $\Lambda \leq \frac{1}{2}(1 - \delta(1 + Ka)/a)$ . The first assumption guarantees that the intermediate states,  $U_i^n$ , satisfy a maximum principle, while the second implies that if  $v_i^0 \geq 0$  and  $u_i^0 \geq U_R(v_i)$  for all  $i$ , then  $v_i^n \geq 0$  for all  $n \geq 0$  and all  $i$ .

We first look at the “point-stimulation” problem discussed in the introduction. We seek the solution of (3.20) satisfying the initial condition

$$(u_i^0, v_i^0) = \begin{cases} (1, 0), & i = 0, \\ (0, 0), & \text{otherwise.} \end{cases} \tag{3.26}$$

As regards this problem we have

**THEOREM 3.1.** *If  $a < \mu < \frac{1}{2}$  and  $0 \leq \Lambda < \frac{1}{2}(1 - \delta(1 + Ka)/a)$ , the solution,  $(u_i^n, v_i^n)$ , of (3.20) and (3.26) converges to a pair of solitary waves, one propagating to the left and one to the right; that is*

$$\lim_{n \rightarrow \infty} (u_{n-|j|}^n, v_{n-|j|}^n) = (\bar{u}_{|j|}, \bar{v}_{|j|}) \tag{3.27}$$

where  $\bar{u}_j$  and  $\bar{v}_j$  are defined by the steady equations

$$\begin{cases} \bar{v}_j = \left(1 - \frac{\Lambda}{1 - \Lambda}\right) \bar{v}_{j-1} + \frac{\Lambda}{1 - \Lambda} \bar{v}_{j-2} + \frac{\delta}{1 - \Lambda} G(\bar{u}_{j-1}, \bar{v}_{j-1}), & j \geq 1, \\ \bar{u}_j = \begin{cases} U_E(\bar{v}_j), & j = 1, 2, \dots, \bar{e}, \\ U_R(\bar{v}_j), & j = \bar{e} + 1, \bar{e} + 2, \dots, \end{cases} \end{cases} \tag{3.28}$$

and the initial conditions

$$(\bar{u}_j, \bar{v}_j) = \begin{cases} (0, 0), & j \leq -1, \\ (1, 0), & j = 0. \end{cases} \tag{3.29}$$

The number  $\bar{e}$  in (3.28) is the largest integer  $e$  such that

$$\bar{v}_j < v_{\max}, \quad 1 \leq j \leq \bar{e}. \tag{3.30}$$

The behavior of the solution to the point stimulation problem is typical of what occurs in one dimension when the initial data has only a finite number of nonzero states. For each mesh point  $i$ ,  $\lim_{n \rightarrow \infty} (u_i^n, v_i^n) = (0, 0)$ . A similar phenomena was observed in the discrete scalar model of §2.

In the remainder of this subsection we consider one dimensional solutions which do not decay as  $n$  approaches infinity. Although our characterization of the data generating such solutions is not as complete as in the discrete

scalar case, we are able to show that the system (3.20) is capable of supporting solutions similar to those obtained in §2.

The nondecaying solutions we obtain are closely related to certain periodic sequences which we now define.

Introduce the functions

$$\begin{cases} \mathcal{V}_R^0(v) = v, & \mathcal{V}_R(v) = v + \delta G(U_R(v), v), & \text{and} & \mathcal{V}_R^j(v) = \mathcal{V}_R(\mathcal{V}_R^{j-1}(v)), \\ \mathcal{V}_E^0(v) = v, & \mathcal{V}_E(v) = v + \delta G(U_E(v), v), & \text{and} & \mathcal{V}_E^j(v) = \mathcal{V}_E(\mathcal{V}_E^{j-1}(v)), \end{cases} \tag{3.31}$$

where again  $G(u, v)$  is given by (3.22). The constraint (3.24) implies that  $\mathcal{V}_R(\cdot)$  is invertible on  $v \geq 0$ . We denote its inverse by  $\mathcal{V}_R^{-1}(\cdot)$  and let

$$\mathcal{V}_R^{-j}(v) = \mathcal{V}_R^{-1}(\mathcal{V}_R^{-(j-1)}(v)). \tag{3.32}$$

We define  $v_\delta \in (0, v_{\max}]$  as the location of the maximum of  $\mathcal{V}_E(\cdot)$  on  $[0, v_{\max}]$ . For the cubic  $f_a$ ,  $v_\delta$  is given by

$$v_\delta = u_\delta(u_\delta - a)(1 - u_\delta) \tag{3.33}$$

where  $u_\delta > u_{\max}$  satisfies

$$3u_\delta^2 - 2(1 + a)u_\delta + a - \delta/(1 - K\delta) = 0 \tag{3.34}$$

and is given by

$$u_\delta = \frac{(1 + a)}{3} + \frac{1}{3} \sqrt{(1 + a)^2 - 3a + \frac{3\delta}{1 - K\delta}}, \tag{3.35}$$

while for the piecewise linear  $f_a$ ,

$$v_\delta \equiv v_{\max} = a(1 - a)^2/(1 + a). \tag{3.36}$$

The constraints on  $K$  imply that

$$0 < u_{\max} - Kv_{\max} \tag{3.37}$$

and hence that

$$v_\delta < v_{\max} < \mathcal{V}_E(v_{\max}) < \mathcal{V}_E(v_\delta). \tag{3.38}$$

In the sequel we shall restrict  $\mathcal{V}_E(\cdot)$  to the interval  $[0, v_\delta]$ , where it is invertible. We denote the inverse by  $\mathcal{V}_E^{-1}(\cdot)$  and define  $\mathcal{V}_E^{-j}(\cdot)$  by

$$\mathcal{V}_E^{-j}(v) = \mathcal{V}_E^{-1}(\mathcal{V}_E^{-(j-1)}(v)). \tag{3.39}$$

For any pair of integers  $e$  and  $r$  satisfying

$$\mathcal{V}_E^{e-1}(0) < v_\delta \quad \text{and} \quad r \geq 1, \tag{3.40}$$

we let

$$\mathcal{V}_{e,r}(v) = \mathcal{V}_R^r(\mathcal{V}_E^e(v)). \tag{3.41}$$

The domain of  $\mathcal{V}_{e,r}(\cdot)$  is

$$\mathcal{D}_e \stackrel{\text{def}}{=} \{v \mid 0 < v < \mathcal{V}_E^{1-e}(v_\delta)\}. \tag{3.42}$$

For any  $e$  and  $r$  as above and  $v_1$  in  $\mathcal{D}_e$  we define the sequence  $(u_j, v_j)(v_1)$ ,  $j = 1, 2, \dots, e + r$ , by

$$(u_j, v_j)(v_1) = \begin{cases} (U_E(\mathcal{V}_E^{\sigma-1}(v_1)), \mathcal{V}_E^{\sigma-1}(v_1)), & 1 \leq j \leq e, \\ (U_R(\mathcal{V}_R^{\sigma-(e+1)}(\mathcal{V}_E^e(v_1))), \mathcal{V}_R^{\sigma-(e+1)}(\mathcal{V}_E^e(v_1))), & e+1 \leq j \leq e+r. \end{cases} \quad (3.43)$$

We will say the sequence  $(u_j, v_j)(v_1)$ ,  $j = 1, 2, \dots, e+r$ , is periodic with period  $e+r$  if and only if

$$\mathcal{V}_{e,r}(v_1) = v_1. \quad (3.44)$$

If this condition holds, we extend the sequence (3.43) to all integers by the periodicity relation

$$(u_{j+e+r}, v_{j+e+r})(v_1) = (u_j, v_j)(v_1). \quad (3.45)$$

The fact that  $0 < \mathcal{V}'_{e,r} < 1$  implies there is at most one periodic sequence for each pair  $(e, r)$ . On the other hand  $\lim_{r \rightarrow \infty} \mathcal{V}_{e,r}(v) = 0$ . Hence such solutions do exist if (3.40) holds and  $r$  is large enough so that  $\mathcal{V}_{e,r}(\mathcal{V}_E^{1-e}(v_\delta)) < \mathcal{V}_E^{1-e}(v_\delta)$ . This follows because  $\mathcal{V}_{e,r}(0) > 0$ .

When  $\Lambda = 0$ , a periodic sequence  $(u_j, v_j)(v_1)$  corresponds to a periodic traveling wave solution  $(u_i^n, v_i^n) = (u_{n+i}, v_{n+i})$  of (3.20) if and only if the following inequalities hold:

$$\begin{aligned} u_{j+1} &< S(\mu u_{j+1} + (1 - 2\mu)u_j + \mu u_{j-1}), \quad 0 \leq j \leq e-1, \\ u_{j+1} &\geq S(\mu u_{j+1} + (1 - 2\mu)u_j + \mu u_{j-1}), \quad e \leq j \leq e+r-1. \end{aligned} \quad (3.46)_j$$

Here, we are making the identifications  $(u_0, v_0) = (u_{e+r}, v_{e+r})$  and  $(u_{-1}, v_{-1}) = (u_{e+r-1}, v_{e+r-1})$ .

Since  $\mu < 1/2$ , the argument of  $S$  is a convex combination of  $u_{j-1}$ ,  $u_j$ , and  $u_{j+1}$  and the inequalities are trivially satisfied for  $2 \leq j \leq e-1$  and  $e+2 \leq j \leq e+r-1$ . For  $e \geq 3$  and  $r \geq 3$  we are left with the four inequalities:

$$\begin{aligned} v_1 &< S(\mu u_1 + (1 - 2\mu)u_{e+r} + \mu u_{e+r-1}), & (3.46)_0 \\ v_2 &< S(\mu u_2 + (1 - 2\mu)u_1 + \mu u_{e+r}), & (3.46)_1 \\ v_{e+1} &\geq S(\mu u_{e+1} + (1 - 2\mu)u_e + \mu u_{e-1}), \quad \text{and} & (3.46)_e \\ v_{e+2} &\geq S(\mu u_{e+2} + (1 - 2\mu)u_{e+1} + \mu u_e). & (3.46)_{e+1} \end{aligned}$$

Our first task is to replace the above inequalities by more manageable ones. We shall assume throughout that  $e \geq 4$  and  $r \geq 4$ .

We investigate  $(3.46)_0$  first. The inequalities  $v_{e+r-1} > v_{e+r} > v_1$  imply that  $U_E(v_{e+r-1}) < u_1$  and  $u_{e+r-1} = U_R(v_{e+r-1}) < u_{e+r}$ . These, when combined with  $dS/du > 0$  and  $\mu < 1/2$  imply that  $(3.46)_0$  is satisfied if

$$v_{e+r-1} < S(\mu U_E(v_{e+r-1}) + (1 - \mu)U_R(v_{e+r-1})). \quad (3.47)_0$$

Moreover,  $(3.47)_0$  holds if

$$a < \mu, \quad \text{and} \quad (3.48)$$

$$v_{e+r-1} < q_1(\mu) \quad (3.49)_0$$

where  $q_1(\mu)$  is the unique solution of

$$q_1 = S(\mu U_E(q_1) + (1 - \mu)U_R(q_1)). \quad (3.50)_0$$

We note that  $dq_1/d\mu > 0$ .

We now look at (3.46)<sub>1</sub>. The inequalities  $v_2 = \mathcal{V}_E(\mathcal{V}_R(v_{e+r})) > v_{e+r} > v_1 = \mathcal{V}_R(v_{e+r})$  imply that  $u_2 = U_E(v_2) < u_1$  and  $U_R(v_2) < U_R(v_{e+r})$ . Thus the arguments applied to (3.46)<sub>0</sub> imply that (3.46)<sub>1</sub> holds if

$$v_2 < S((1 - \mu)U_E(v_2) + \mu U_R(v_2)). \tag{3.47}_1$$

This inequality is satisfied if

$$v_2 < q_2(\mu) \tag{3.49}_1$$

where  $q_2(\mu)$  is the unique solution of

$$q_2 = S((1 - \mu)U_E(q_2) + \mu U_R(q_2)). \tag{3.50}_1$$

It is easily checked that  $dq_2/d\mu < 0$  and

$$q_1(\mu) < q_2(\mu) \tag{3.51}$$

for  $a < \mu < 1/2$ .

Similar arguments applied to (3.46)<sub>e</sub> and (3.46)<sub>e+1</sub> imply that they are valid if

$$v_{e-1} > q_2(\mu), \tag{3.49}_e$$

and

$$v_e > q_1(\mu). \tag{3.49}_{e+1}$$

What remains to be shown is there are parameter values  $(a, \delta, K, \mu)$ , integers  $e$  and  $r$ , and periodic sequences  $(u_j, v_j)(v_1)$  such that (3.46)<sub>j</sub>,  $j = 0, 1, e$ , and  $e + 1$  hold. We choose  $a \in (0, 1/2)$ ,  $K \geq 0$  and small, and  $a < \mu < 1/2$  and fix them. We choose  $0 < \delta < a/(1 + Ka)$  so that  $\mathcal{V}_E^2(q_2) < v_\delta$  and fix it. It is now a simple matter to show there is a range of values of  $e$  and  $r$  such that any periodic sequence with these indices satisfies (3.49)<sub>j</sub>,  $j = 0, 1, e$ , and  $e + 1$ , and hence the desired inequalities (3.46)<sub>j</sub>,  $j = 0, 1, e$ , and  $e + 1$ .

We now turn to the case where  $\Lambda > 0$ . We let  $(u_j, v_j)(v_1)$ ,  $-\infty < j < \infty$ , be a periodic sequence as defined by (3.43), (3.44) and (3.45). We assume that  $\mu < 1/2$  and that

$$\begin{aligned} u_{j+1} &< S(\mu u_{j+1} + (1 - 2\mu)u_j + \mu u_{j-1}), & 0 < j < e - 1 \\ u_{j+1} &> S(\mu u_{j+1} + (1 - 2\mu)u_j + \mu u_{j-1}), & e < j < e + r - 1. \end{aligned} \tag{3.52}$$

We let

$$V_j(d) = \{q \mid |q - v_j| \leq d\}, \quad 1 \leq j \leq e + r, \tag{3.53}$$

$$V(d) = \{q \in R^{e+r} \mid q_j \in V_j(d), \quad 1 \leq j \leq e + r\}, \tag{3.54}$$

and choose  $d > 0$  such that the following inequalities hold:

$$\left\{ \begin{aligned} d &< \min \left[ \min_{1 \leq j < e+r} \left| \frac{v_{j+1} - v_j}{2} \right|, v_\delta - v_e, \mathcal{V}_E(v_\delta) - v_{e+1}, v_1 \right], \\ q_{j+1} &< S(\mu p_{j+1} + (1 - 2\mu)p_j + \mu p_{j-1}), & 0 < j < e - 1, \\ q_{j+1} &> S(\mu p_{j+1} + (1 - 2\mu)p_j + \mu p_{j-1}), & e < j < e + r - 1. \end{aligned} \right. \tag{3.55}$$



with

$$p_j = \begin{cases} U_E(q_j), & 1 \leq j \leq e, \\ U_R(q_j), & e + 1 \leq j \leq e + r, \end{cases} \tag{3.56}$$

for all  $q_j \in V_j(d)$ ,  $1 \leq j \leq e + r$ . For any  $q \in V(d)$ , we let  $T(q) \in R^{e+r}$  be defined by

$$T_j(q) = q_{j-1} + \delta G(p_{j-1}, q_{j-1}) + \Lambda(q_j - 2q_{j-1} + q_{j-2}), \quad 1 \leq j \leq e + r. \tag{3.57}$$

Here,  $q_0 = q_{e+r}$  and  $q_{-1} = q_{e+r-1}$ . The inequalities

$$0 < d^{\mathcal{V}_E}/dv = 1 - \delta K + \delta U'_E(v) < 1, \quad 0 < v < v_\delta,$$

and

$$0 < d^{\mathcal{V}_R}/dv = 1 - \delta K + \delta U'_R(v) < 1, \quad 0 < v < \mathcal{V}_E(v_\delta)$$

guarantee that for

$$\Lambda < \frac{\delta}{4} (K + \min(|U'_E(0)|, |U'_R(\mathcal{V}_E(v_\delta))|)), \tag{3.58}$$

$T$  maps  $V(d)$  into  $V(d)$  and satisfies

$$\|T(q) - T(q')\| \leq M\|q - q'\| \tag{3.59}$$

for some  $M$  in  $(0, 1)$  and all pairs  $q, q'$  in  $V(d)$ . In the above inequality,

$$\|x\| = \max_{1 \leq i \leq e+r} |x_i|. \tag{3.60}$$

Thus  $T$  is a contraction on  $V(d)$  and hence has a unique fixed point. Moreover, if  $q \in V(d)$  is a fixed point of  $T$ , then  $(u_i^n, v_i^n) = (p_{(i+n) \bmod (e+r)}, q_{(i+n) \bmod (e+r)})$  is an  $e + r$  periodic traveling wave solution of (3.20).

An immediate consequence of the preceding computations is

**THEOREM 3.2.** *Let  $(u_j, v_j)(v_1)$  be a periodic sequence (see (3.43)–(3.45)),  $\mu < 1/2$  be such that (3.52) holds,  $d > 0$  be such that (3.55) holds, and  $\Lambda$  such that (3.58) is satisfied. Then, the solution,  $(u_i^n, v_i^n)$ , to (3.20) taking on the data  $(u_i^0, v_i^0)$  with  $v_i^0 \in V_i(d)$ ,  $i = 1, 2, \dots, e + r$ ,*

$$u_i^0 = \begin{cases} U_E(v_i^0), & i = 1, 2, \dots, e, \\ U_R(v_i^0), & i = e + 1, e + 2, \dots, e + r, \end{cases}$$

and

$$(u_{i+e+r}^0, v_{i+e+r}^0) = (u_i^0, v_i^0)$$

satisfies

$$v_{i-n}^n \in V_i(d), \quad i = 1, 2, \dots, e + r,$$

$$u_{i-n}^n = \begin{cases} U_E(v_{i-n}^n), & i = 1, 2, \dots, e, \\ U_R(v_{i-n}^n), & i = e + 1, e + 2, \dots, e + r, \end{cases}$$

and

$$(u_{i+e+r}^n, v_{i+e+r}^n) = (u_i^n, v_i^n).$$

Moreover,  $\lim_{n \rightarrow \infty} v_{i-n}^n = q_i, i = 1, 2, \dots, e + r$ , where  $q$  is the unique fixed point of  $T$  in  $V(d)$ .

The periodic sequences may also be used to generate ‘‘caterpillar’’ wave solutions of (3.20). We again let  $(u_j, v_j)(v_1), -\infty < j < \infty$ , be a periodic sequence as defined by (3.43), (3.44) and (3.45).

Our interest is in the solution of (3.20) satisfying the initial condition

$$\begin{cases} (u_i^0, v_i^0) = (u_i, v_i)(v_1), & 1 \leq i \leq e + r + 1 - p, \\ (u_{i+e+r+1-p}^0, v_{i+e+r+1-p}^0) = (u_i^0, v_i^0) \end{cases} \tag{3.61}$$

where  $1 \leq p \leq e$ .

We treat the case  $\Lambda = 0$  first. We seek parameter constraints so that the solution of  $(3.20)_{\Lambda=0}, (3.61)$ , is given by

$$(u_i^n, v_i^n) = (u, v)_{(n+i \bmod (e+r+1-p)) \bmod (e+r)} \tag{3.62}$$

and hence satisfies the periodicity relations

$$(u_i^{n+e+r}, v_i^{n+e+r}) = (u_{e+r+1-p+i}^n, v_{e+r+1-p+i}^n) = (u_i^n, v_i^n). \tag{3.63}$$

An elementary analysis of the difference equations (3.20) shows that the solution is given by (3.62) if and only if the following inequalities are satisfied:

$$\begin{aligned} v_{j+1} &< S(\mu u_{j+1} + (1 - 2\mu)u_j + \mu u_{j-1}) & 0 \leq j \leq e - 1, \\ v_{j+1} &< S(\mu u_{j+p} + (1 - 2\mu)u_j + \mu u_{j-1}) & 0 \leq j \leq e - 1, \\ v_{j+1} &< S(\mu u_{j+1} + (1 - 2\mu)u_j + \mu u_{j-p}) & 0 \leq j \leq e - 1, \\ v_{j+1} &> S(\mu u_{j+1} + (1 - 2\mu)u_j + \mu u_{j-1}) & e \leq j \leq e + r - 1, \\ v_{j+1} &> S(\mu u_{j+p} + (1 - 2\mu)u_j + \mu u_{j-1}) & e \leq j \leq e + r - 1, \\ v_{j+1} &> S(\mu u_{j+1} + (1 - 2\mu)u_j + \mu u_{j-p}) & e \leq j \leq e + r - 1. \end{aligned}$$

That the parameters may be tuned so that the last inequalities hold is left to the reader.

The existence of ‘‘caterpillar’’ waves for  $\Lambda > 0$  follows from a perturbation argument similar to that employed in establishing the existence of spatially periodic traveling wave solutions of (3.20) when  $\Lambda > 0$ .

We conclude this section on one-dimensional solutions with some examples of periodic sequences and the solutions of (3.20) they generate. In these examples we have chosen  $K = \Lambda = 0$  and  $f_a(u) = u(u - a)(1 - u)$ . Then,  $\sqrt[3]{E}(v) = v + \delta U_E(v)$  and  $\sqrt[3]{R}(v) = v + \delta U_R(v)$  where  $U_E(v), U_I(v)$ , and  $U_R(v)$  are the roots of the cubic  $u(u - a)(1 - u) = v$  and are defined in (3.19). For fixed values of  $a$  and  $\delta$  we let

$$\begin{aligned} e_{\max} &= e_{\max}(a, \delta) \\ &= \{\text{largest integer } e \geq 1 \text{ such that } \sqrt[3]{E}^e(0) \leq v_\delta\}. \end{aligned} \tag{3.64}$$

We will restrict our attention to integers  $e \leq e_{\max}$  and  $r \geq r_{\min}(e)$  where

$$r_{\min}(e) = \{ \text{smallest integer } r \geq 1 \text{ such that } \sqrt[e]{v_R}(\sqrt[e]{v_E}(v_\delta)) < \sqrt[e]{v_E^{1-e}}(v_\delta) \}. \tag{3.65}$$

The following table shows  $e_{\max} = e_{\max}(a, \delta)$  and  $r_{\min}(e)$  for  $e = 1$  and  $e = e_{\max}$  in the format  $e_{\max}/r_{\min}(1), r_{\min}(e_{\max})$ . This table and the subsequent examples were calculated to an absolute precision of  $10^{-8}$  using APL on the SUNY at Buffalo Cyber 173. Floating point numbers quoted have been rounded to 4 decimal places.

TABLE

$\delta/a \backslash a$	.1	.2	.3	.4
.1	14/4, 79	6/5, 46	3/6, 26	2/9, 26
.2	7/4, 35	3/5, 18	2/6, 17	1/8, 8
.3	5/4, 25	2/5, 12	1/6, 6	1/8, 8
.4	4/4, 20	2/5, 11	1/6, 6	1/7, 7
.5	3/4, 13	1/5, 5	1/6, 6	1/7, 7

In these examples we take  $a = 0.1, \delta = 0.03, e = 4, r = 20 > r_{\min}(4) = 17$ . The root  $v_1$  of  $\sqrt[4]{v_{4,20}}(v_1) = v_1$  is 0.0174 and the corresponding 24-periodic sequence is

$$\left\{ \begin{array}{l} u = (0.9798, \quad 0.9409, \quad 0.8944, \quad 0.8334, \quad -0.2700, \quad -0.2609, \\ \quad -0.2518, \quad -0.2427, \quad -0.2335, \quad -0.2243, \quad -0.2151, \quad -0.2058, \\ \quad -0.1965, \quad -0.1872, \quad -0.1779, \quad -0.1685, \quad -0.1592, \quad -0.1498, \\ \quad -0.1405, \quad -0.1312, \quad -0.1220, \quad -0.1129, \quad -0.1038, \quad -0.0948) \\ v = (0.0174, \quad 0.0468, \quad 0.0750, \quad 0.1018, \quad 0.1268, \quad 0.1187, \\ \quad 0.1109, \quad 0.1034, \quad 0.0961, \quad 0.0891, \quad 0.0823, \quad 0.0759, \\ \quad 0.0697, \quad 0.0638, \quad 0.0582, \quad 0.0529, \quad 0.0478, \quad 0.0430, \\ \quad 0.0385, \quad 0.0343, \quad 0.0304, \quad 0.0267, \quad 0.0233, \quad 0.0202). \end{array} \right. \tag{3.66}$$

We shall show there are ranges on the parameter  $\mu$  so that this sequence generates a periodic traveling wave and a ‘‘caterpillar’’ wave with  $p = 2$  (see (3.63)).

Our first task is to show there is a range of values of  $\mu$  in the interval  $a = 0.1 < \mu < 0.5$  such that the sequence

$$(u_i^n, v_i^n) = (u_{(i+n) \bmod 24}, v_{(i+n) \bmod 24}) \tag{3.67}$$

solves (3.20). Here  $(u_j, v_j), 1 \leq j \leq 24$ , are the elements of the sequence (3.66).

If the sequence (3.66) is to be a solution and  $n$  and  $i$  are such that

$(u_i^n, v_i^n) = (u_{24}, v_{24})$ , then  $(u_{i-1}^n, v_{i-1}^n) = (u_{23}, v_{23})$  and  $(u_{i+1}^n, v_{i+1}^n) = (u_1, v_1)$ . To be assured that  $(u_i^{n+1}, v_i^{n+1}) = (u_1, v_1)$ ,  $\mu$  must satisfy

$$u_{24} + \mu(u_{23} - 2u_{24} + u_1) > U_I(v_1) = 0.2062, \tag{3.68}$$

or equivalently

$$\mu > 0.2825. \tag{3.69}$$

It is easily verified that for any  $\mu$  satisfying  $0.2825 < \mu < 0.5$ , cells in the excited states  $(u_i, v_i)$ ,  $1 < i < 3$ , will remain excited and advance to  $(u_{i+1}, v_{i+1})$  at the next time level. A cell in the excited state  $(u_4, v_4)$  must jump down to the refractory state  $(u_5, v_5)$  at the next instant since  $v_5 > v_{\max} = 0.1252$ . For values of  $\mu$  satisfying  $0.2825 < \mu < 0.5$ , cells in the refractory states  $(u_i, v_i)$ ,  $5 < i < 23$ , remain refractory and advance to  $(u_{i+1}, v_{i+1})$  at the next instant.

Hence, we have the result that *for any value of  $\mu$  satisfying  $0.2825 < \mu < 0.5$ , the periodic sequence described by (3.67) generates a 24 periodic traveling wave solution of (3.20).*

We conclude by showing there is a range of parameter values  $\mu$  such that the sequence

$$(u_i^n, v_i^n) = (u_{(n+i \bmod 23) \bmod 24}, v_{(n+i \bmod 23) \bmod 24}) \tag{3.70}$$

solves (3.20). If  $n$  and  $i$  are such that  $(u_i^n, v_i^n) = (u_{24}, v_{24})$ , then

$$((u_{i-1}^n, v_{i-1}^n), (u_{i+1}^n, v_{i+1}^n)) = \begin{cases} ((u_{23}, v_{23}), (u_1, v_1)), & \text{or} \\ ((u_{22}, v_{22}), (u_1, v_1)), & \text{or} \\ ((u_{23}, v_{23}), (u_2, v_2)). \end{cases} \tag{3.71}$$

To be assured that  $(u_i^{n+1}, v_i^{n+1}) = (u_1, v_1)$ ,  $\mu$  must satisfy the lower bound

$$\mu > \max(0.2825, 0.2849, 0.2932) = 0.2932. \tag{3.72}$$

Similarly, if  $n$  and  $i$  are such that  $(u_i^n, v_i^n) = (u_{23}, v_{23})$ , then

$$((u_{i-1}^n, v_{i-1}^n), (u_{i+1}^n, v_{i+1}^n)) = \begin{cases} ((u_{22}, v_{22}), (u_{24}, v_{24})), & \text{or} \\ ((u_{21}, v_{21}), (u_{24}, v_{24})), & \text{or} \\ ((u_{22}, v_{22}), (u_1, v_1)). \end{cases} \tag{3.73}$$

To be assured that  $(u_i^{n+1}, v_i^{n+1}) = (u_{24}, v_{24})$ , we must constrain  $\mu$  to satisfy the upper bound

$$\mu < (U_I(v_1) - u_{23}) / (u_{22} - 2u_{23} + u_1) = 0.2999. \tag{3.74}$$

The situation when

$$(u_j^n, v_j^n) = (u_j, v_j), \quad 1 < j < 22, \tag{3.75}$$

and

$$((u_{i-1}^n, v_{i-1}^n), (u_{i+1}^n, v_{i+1}^n)) = \begin{cases} ((u_{(j-1) \bmod 24}, v_{(j-1) \bmod 24}), (u_{j+1}, v_{j+1})), & \text{or} \\ ((u_{(j-2) \bmod 24}, v_{(j-2) \bmod 24}), (u_{j+1}, v_{j+1})), & \text{or} \\ ((u_{(j-1) \bmod 24}, v_{(j-1) \bmod 24}), (u_{j+2}, v_{j+2})) \end{cases} \tag{3.76}$$

is essentially the same as in the previous example. That is, for any  $\mu$  in  $(0.2932, 0.2999)$ ,  $(u_i^{n+1}, v_i^{n+1}) = (u_{j+1}, v_{j+1})$ . Thus the sequence defined in (3.70) is a solution of (3.20) for any  $\mu$  in the above interval.

3.4 *Two dimensional problems.* We conclude with a brief section on two dimensional problems. The governing equations are

$$\begin{cases} U_{ij}^{n+1} = \mu(u_{i-1,j}^n + u_{i,j-1}^n + u_{i+1,j}^n u_{i,j+1}^n) + (1 - 4\mu)u_{ij}^n \\ v_{ij}^{n+1} = \Lambda(v_{i-1,j}^n + v_{i,j-1}^n + v_{i+1,j}^n + v_{i,j+1}^n) \\ \quad + (1 - 4\Lambda)v_{ij}^n + \delta G(u_{ij}^n, v_{ij}^n), \text{ and} \\ u_{ij}^{n+1} = \begin{cases} U_E(v_{ij}^{n+1}), & v_{ij}^{n+1} < S(U_{ij}^{n+1}), \\ U_R(v_{ij}^{n+1}), & v_{ij}^{n+1} \geq S(U_{ij}^{n+1}). \end{cases} \end{cases} \tag{3.21}$$

Again  $F$  and  $G$  are given by (3.22),  $K$  is chosen small enough so that  $(0, 0)$  is the unique solution of  $(F, G) = (0, 0)$ ,  $0 < \delta < a/(1 + Ka)$ , and  $0 < a \leq 1/2$ .

We shall insist that  $\mu \leq 1/4$  and  $\Lambda \leq \frac{1}{4}(1 - \delta(1 + Ka)/a)$ . The first constraint guarantees that the intermediate states,  $U_{ij}^{n+1}$ , satisfy a maximum principle, while the second implies that if  $v_{ij}^0 \geq 0$  and  $u_{ij}^0 \geq U_R(v_{ij}^0)$  for all  $i$  and  $j$ , then  $v_{ij}^n \geq 0$  for all  $n \geq 0$  and all  $i$  and  $j$ .

We first look at the point stimulation problem. We seek a solution of (3.21) satisfying the initial condition

$$(u_{ij}^0, v_{ij}^0) = \begin{cases} (1, 0), & (i,j) = (0, 0), \\ (0, 0), & \text{otherwise.} \end{cases} \tag{3.79}$$

As regards the solution of this problem we have

**THEOREM 3.3.** *If  $a < \mu < 1/4$  and  $\Lambda = 0$ , the solution,  $(u_{ij}^n, v_{ij}^n)$ , converges to a steady outgoing wave; that is*

$$\lim_{\substack{n \rightarrow \infty \\ |i|+|j|=n-r}} (u_{ij}^n, v_{ij}^n) = (\bar{u}_r, \bar{v}_r) \tag{3.80}$$

where  $\bar{u}_r$  and  $\bar{v}_r$  are defined by the steady equations

$$\begin{cases} \bar{v}_r = \bar{v}_{r-1} + \delta G(\bar{u}_{r-1}, \bar{v}_{r-1}), \text{ and} \\ \bar{u}_r = \begin{cases} U_E(\bar{v}_r), & r = 1, 2, \dots, \bar{e}, \\ U_R(\bar{v}_r), & r = \bar{e} + 1, \bar{e} + 2, \dots, \end{cases} \end{cases} \tag{3.81}$$

and the initial conditions

$$(\bar{u}_r, \bar{v}_r) = \begin{cases} (0, 0), & r \leq -1, \\ (1, 0), & r = 0. \end{cases} \tag{3.82}$$

The number  $\bar{e}$  in (3.81) is the largest integer  $e$  such that

$$\bar{v}_r \leq v_{\max}, \quad 1 \leq r \leq \bar{e}. \tag{3.83}$$

When  $0 < \Lambda \leq \frac{1}{4}(1 - \delta(1 + Ka)/a)$ , the data guarantees an outgoing wave, but the solution is not a simple function of  $|i| + |j|$ . Be that as it may, we still have

$$\lim_{\substack{n \rightarrow \infty \\ |i| + |j| = n}} (u_{i,j}^n, v_{i,j}^n) = (1, 0). \quad (3.84)$$

The system (3.20) also supports rotating spiral solutions of the type described in the introduction. When  $\Lambda = 0$ , some of these may be written down in terms of the periodic sequences of the previous section. Each point  $(i, j)$  runs through the given sequence and what must be checked is that the inequalities (3.21)<sub>3</sub> are satisfied. As in the example of a "caterpillar" wave, one must demonstrate there is a range of the parameter  $\mu$  such that the given spiral pattern satisfies the requisite inequalities.

Spiral patterns may also be generated as solutions to the initial value problem for (3.21) with initial data containing no spirals at  $t = 0$ . We have worked out such an example for the parameter values  $a = 0.1$ ,  $\delta = 0.02$ ,  $\mu = 0.15$ , and  $\Lambda = K = 0$ , when  $f_a$  is the piecewise linear function defined in (3.23). We set up the initial conditions

$$(u_{i,j}^0, v_{i,j}^0) = \begin{cases} (0, 0), & 1 \leq i \leq 60, 2 \leq j \leq 60, \\ (1, 0), & 1 \leq i \leq 60, j = 1, \end{cases} \quad (3.85)$$

on a 60 by 60 grid.

At each time step, the boundary conditions

$$\begin{cases} (u_{0,j}^n, v_{0,j}^n) = (u_{1,j}^n, v_{1,j}^n), (u_{61,j}^n, v_{61,j}^n) = (u_{60,j}^n, v_{60,j}^n) \\ (u_{i,0}^n, v_{i,0}^n) = (u_{i,1}^n, v_{i,1}^n), (u_{i,61}^n, v_{i,61}^n) = (u_{i,60}^n, v_{i,60}^n), \\ i, j = 1, \dots, 60, \end{cases} \quad (3.86)$$

were imposed. Since the spiral will develop from the center of the grid, it will be apparent that the spiral in its initial stages is not affected by the form of the boundary conditions chosen.

For  $1 \leq n \leq 29$ , we evaluated  $(u_{i,j}^n, v_{i,j}^n)$  numerically using equations (3.21) and (3.86). Printer plots of the solution at each time step were produced, with the symbol ' + ' in location  $(i, j)$  indicating a pair  $(u_{i,j}^n, v_{i,j}^n)$  in an excited state. A traveling wave of width 4 was observed, moving in the positive  $j$  direction.

Before using (3.21) for  $n = 29$ , however, we arbitrarily cut the wave in half by redefining

$$u_{i,j}^{29} = v_{i,j}^{29} = 0, \quad 1 \leq i \leq 31, 1 \leq j < 60. \quad (3.87)$$

With the modified values  $(u_{i,j}^{29}, v_{i,j}^{29})$  regarded as new initial conditions, we evaluated  $(u_{i,j}^n, v_{i,j}^n)$  for  $30 \leq n \leq 60$  by means of (3.21) and (3.86).

The spiral that develops is shown for  $n = 35, 45, 55$  in Figures 3.3, 3.4, and 3.5. The horizontal band is the remnant of the original traveling wave and moves upwards (the positive  $j$  direction) at a rate of 1 unit per time step. At time  $n = 35$ , the wake of the traveling wave has not been refractory long enough to be re-excited by the spiral. The first invasion of this wake by the spiral occurs at  $n = 40$ . At  $n = 45$ , the spiral is ready to invade its own wake, but must wait until  $n = 50$  before the wake is ready. By  $n = 55$ , the emerging spiral pattern has become quite evident.

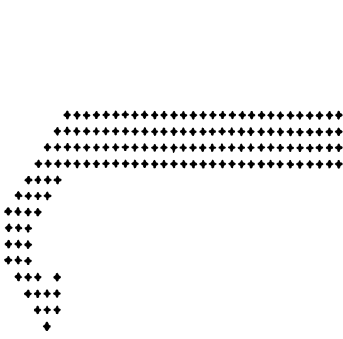


FIGURE 3.3  
Spiral wave at  $n = 35$

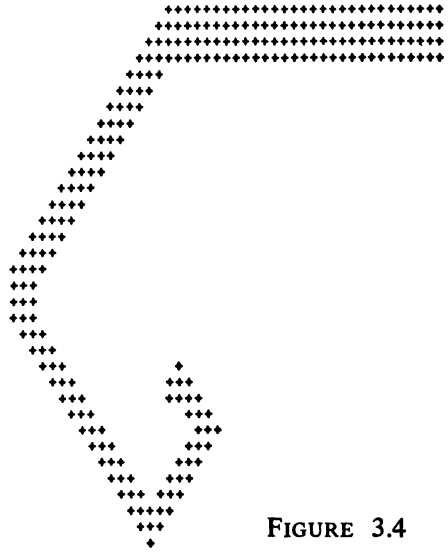


FIGURE 3.4  
Spiral wave at  $n = 45$

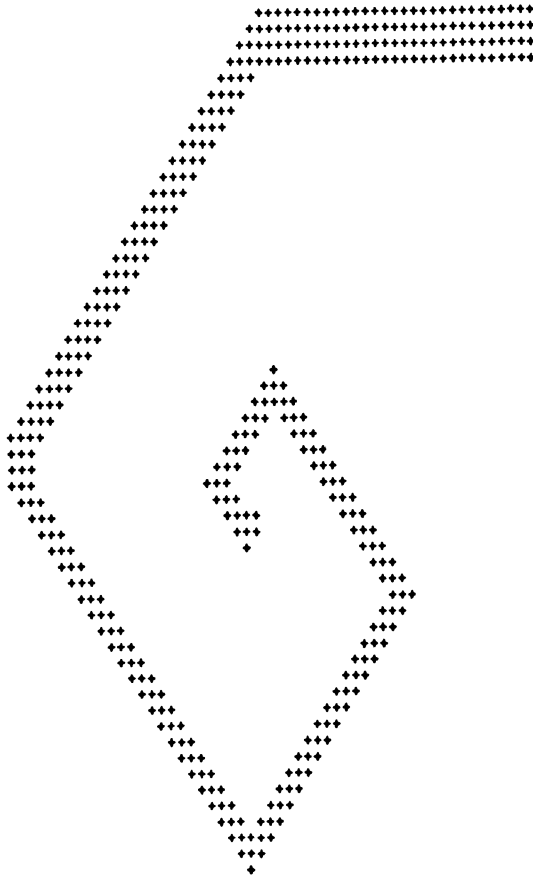


FIGURE 3.5. Spiral wave at  $n = 45$

## REFERENCES

1. R. FitzHugh, *Mathematical models of excitation and propagation in nerve*, Biological Engineering, H. P. Schwan (ed.), McGraw-Hill, New York, 1969.
2. J. M. Greenberg and S. P. Hastings, *Spatial patterns for discrete models of diffusion in excitable media*, SIAM J. Appl. Math. **34** (1978).
3. J. M. Greenberg, C. Greene, and S. P. Hastings, *A combinatorial problem arising in the study of reaction-diffusion equations*, SIAM J. Appl. Math. (to appear).
4. S. P. Hastings, *Some mathematical problems from neurobiology*, Amer. Math. Monthly **82** (1975), 881-895.
5. J. Nagumo, S. Yoshizawa, and S. Arimoto, *Bistable transmission lines*, IEEE Trans. Comm. Tech. **12** (1965), 400.
6. L. V. Reshodko, and S. Bures, *Computer simulation of reverberating spreading depression in a network of cell automata*, Biol. Cybernet. **18** (1975), 181-190.
7. N. Wiener and A. Rosenblueth, *The mathematical formulation of the problem of conduction of impulses in a network of connected excitable elements, specifically in cardiac muscle*, Arch. Inst. Cardiol. Mexico **16** (1946), 205-265.
8. A. T. Winfree, *Wavelike activity in biological and biochemical media*, Lecture Notes in Biomathematics, P. van den Driessche (ed.), Springer-Verlag, Berlin, 1974, p. 241.

DEPARTMENT OF MATHEMATICS, STATE UNIVERSITY OF NEW YORK AT BUFFALO, BUFFALO, NEW YORK 14214